

Phosphorylation of Serine 106 in Asef2 Regulates Cell Migration and Adhesion Turnover

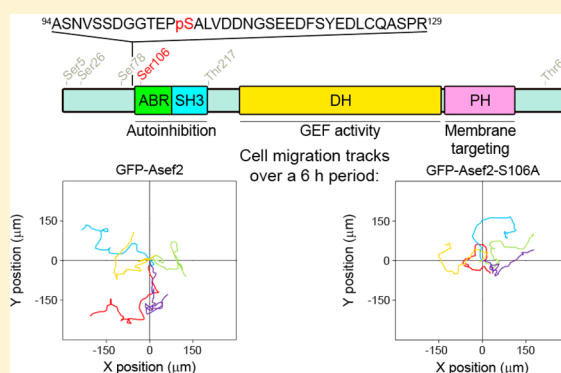
J. Corey Evans,^{†,○} Kelly M. Hines,^{‡,§,||,○} Jay G. Forsythe,^{‡,§,||,○} Begum Erdogan,[†] Mingjian Shi,[†] Salisha Hill,[‡] Kristie L. Rose,^{‡,¶} John A. McLean,^{*,‡,§,||} and Donna J. Webb^{*,†,||,●}

[†]Department of Biological Sciences and Vanderbilt Kennedy Center for Research on Human Development, [‡]Department of Chemistry, [§]Vanderbilt Institute for Chemical Biology (VICB), ^{||}Vanderbilt Institute for Integrative Biosystems Research and Education (VIIBRE), [‡]Mass Spectrometry Research Center, [¶]Department of Biochemistry, and [●]Department of Cancer Biology, Vanderbilt University, Nashville, Tennessee 37235, United States

Supporting Information

ABSTRACT: Asef2, a 652-amino acid protein, is a guanine nucleotide exchange factor (GEF) that regulates cell migration and other processes via activation of Rho family GTPases, including Rac. Binding of the tumor suppressor adenomatous polyposis coli (APC) to Asef2 is known to induce its GEF activity; however, little is currently known about other modes of Asef2 regulation. Here, we investigated the role of phosphorylation in regulating Asef2 activity and function. Using high-resolution mass spectrometry (MS) and tandem mass spectrometry (MS/MS), we obtained complete coverage of all phosphorylatable residues and identified six phosphorylation sites. One of these, serine 106 (S106), was particularly intriguing as a potential regulator of Asef2 activity because of its location within the APC-binding domain. Interestingly, mutation of this serine to alanine (S106A), a non-phosphorylatable analogue, greatly diminished the ability of Asef2 to activate Rac, while a phosphomimetic mutation (serine to aspartic acid, S106D) enhanced Rac activation. Furthermore, expression of these mutants in HT1080 cells demonstrated that phosphorylation of S106 is critical for Asef2-promoted migration and for cell-matrix adhesion assembly and disassembly (adhesion turnover), which is a process that facilitates efficient migration. Collectively, our results show that phosphorylation of S106 modulates Asef2 GEF activity and Asef2-mediated cell migration and adhesion turnover.

KEYWORDS: mass spectrometry, phosphoproteomics, phosphorylation site mapping, guanine nucleotide exchange factors, Rho family GTPases, Rac, cell migration, adhesion dynamics



INTRODUCTION

Cell migration is a complex, actin-dependent process that plays a central role in embryonic development and wound healing.¹ The tightly controlled signaling pathways that mediate cell migration can be altered in pathological states, such as tumor metastasis and atherosclerosis.^{2,3} Cell migration involves several canonical steps: the extension of actin-rich protrusions, the assembly of nascent adhesions at the leading edge, the translocation of the cell body, and the retraction of the rear of the cell.⁴ The assembly of leading edge adhesions, which are sites of contact between cells and the extracellular matrix, stabilizes protrusions and provides traction to propel the forward movement of cells.^{4–6} Once formed, nascent adhesions can disassemble, or they can continue to grow into larger, more stable adhesions.^{7,8} The constant assembly and disassembly of leading edge adhesions, termed adhesion turnover, is crucial for efficient cell migration^{7,9} but not well understood on a molecular level.

Small GTPases that comprise the Rho family, including Rho, Rac, and Cdc42, are key modulators of cell migration through

their ability to regulate processes underlying migration, such as adhesion assembly, disassembly, and maturation.^{1,10–12} Rho family GTPases, like other small GTPases, function by cycling between a GTP-bound active form and a GDP-bound inactive form.¹³ This cycling is dependent on GEFs that catalyze the exchange of GDP for GTP and GTPase activating proteins (GAPs), which promote the hydrolysis of GTP.^{14–17} Upon activation by GEFs, the Rho GTPases, in turn, activate a series of downstream effector proteins that regulate adhesion and actin dynamics.^{12,18,19} While the role of the Rho GTPases in regulating cell migration has been studied, less is known about the function of the various GEFs and GAPs in modulating migration and its underlying processes.

Asef2 is a recently discovered GEF that has been implicated in the regulation of cell migration.^{20–22} This 652-amino acid protein is composed of several functional domains: an APC-binding region (ABR), a Src homology 3 (SH3) domain, a Dbl

Received: February 12, 2014

Published: May 29, 2014

homology (DH) domain, and a pleckstrin homology (PH) domain.²⁰ The DH domain mediates GTP exchange for Rac and Cdc42, while the PH domain is most likely involved in membrane localization.^{20–22} The ABR and SH3 domains work in concert to regulate Asef2 activity.²⁰ Asef2 exists in an autoinhibited conformation that prevents nucleotide exchange by the DH domain; once the tumor suppressor APC binds to the tandem ABR and SH3 domains, Asef2 undergoes a conformational change that stimulates its GEF activity.^{20,23,24} While the mechanism of APC binding to Asef2 and relieving autoinhibition has been studied,²⁰ little is currently known about other potential modes of Asef2 regulation. For example, post-translational modification of Asef2 is one possible avenue of modulating its activity and function. The addition of chemical moieties, such as acetyl, phosphate, or glycosyl groups, to a protein is a common mechanism for altering its conformation, localization, and activity.²⁵ Indeed, it has previously been shown that phosphorylation of GEFs is necessary for proper function.^{26–28} These data point to a possible role for phosphorylation in regulating Asef2 activity and function.

Here, we describe the identification of phosphorylation sites in Asef2 using a liquid chromatography–mass spectrometry (LC–MS) approach consisting of high-mass-resolution Orbitrap MS, data-dependent tandem MS (MS/MS), multiple protease and denaturing strategies, and bioinformatics-based peptide and protein assignments.²⁹ This methodology yielded a 94.5% sequence coverage and identified six sites of phosphorylation. The portion of the sequence that was not covered does not contain serine, threonine, or tyrosine residues; therefore, 100% coverage of possible phosphorylatable sites was achieved. The majority of these sites are clustered in the N-terminus of Asef2; one site (S106) is located in the ABR domain,^{20,21} suggesting that it could regulate Asef2 activity. Indeed, we show that S106 phosphorylation is crucial for Asef2-promoted Rac activation, cell migration, and adhesion turnover, pointing to a new regulatory mechanism for Asef2 activity and function.

MATERIALS AND METHODS

Reagents and Plasmids

Mouse IgG agarose, FLAG M2-agarose affinity gel, FLAG peptide (DYKDDDDK), FLAG monoclonal antibody (clone M2), and fibronectin were obtained from Sigma (St. Louis, MO). Sodium vanadate was purchased from Fischer Scientific (Fairlawn, NJ), and calyculin A was obtained from EMD Millipore (Billerica, MA). Peroxovanadate was prepared as previously described.²⁹ Glutathione sepharose beads were purchased from GE Healthcare Life Sciences (Piscataway, NJ). Phosphoserine polyclonal antibody (catalog number 61-8100) was obtained from Life Technologies (Grand Island, NY). GFP-Asef2 was generated by cloning human Asef2 (accession number: NM_153023.2) into EGFP-C3 vector (Clontech, Mountain View, CA) at *EcoRI* sites as previously described.²² FLAG-CFP was prepared as previously described,²⁹ and FLAG-CFP-Asef2 was generated by inserting human Asef2 into the FLAG-CFP vector at *EcoRI* sites. Asef2 serine 106 mutants were created via site-directed mutagenesis using the following primers: serine 106 to alanine (Asef2-S106A), forward (5'-GGTACTGAGCCCCTGCCTT-AGTGGAT-3') and reverse (5'-ATCCACTAAGGCAGC-GGGCTCAGTACC-3'); serine 106 to aspartic acid (Asef2-S106D), forward (5'-GGTACTGAGCCCCTGCCTT-

AGTGGAT-3') and reverse (5'-ATCCACTAAGGCATC-GGGCTCAGTACC-3'). mCherry-paxillin was a generous gift from Steve Hanks (Vanderbilt University, Nashville, TN).

Cell Culture and Transfection

HT1080 fibrosarcoma cells and human embryonic kidney 293 (HEK293) cells were cultured in Dulbecco's Modified Eagle medium (DMEM, Life Technologies, Grand Island, NY), which was supplemented with 10% fetal bovine serum (FBS; Thermo Scientific, Waltham, MA) and penicillin/streptomycin (Life Technologies, Grand Island, NY). These cells were maintained in an incubator with 5% carbon dioxide (CO₂) at 37 °C. Cells were transiently transfected with appropriate cDNAs using Lipofectamine 2000 (Life Technologies, Grand Island, NY) according to the manufacturer's instructions.

Protein Purification

HEK293 cells were cultured in eight 150 mm dishes (Corning, Tewksbury, MA) for 24 h and then transfected with FLAG-CFP-Asef2 cDNA (12 µg per dish). After approximately 40 h, cells were treated with 1 mM peroxovanadate and 50 nM calyculin A for 10 min and then extracted with 25 mM Tris, 137 mM NaCl, 1% NP-40, 10% glycerol, and 2 mM EDTA (pH 7.4) containing a protease inhibitor cocktail (Sigma, St. Louis, MO; catalogue number P2714) for 30 min on ice. The lysate was precleared with mouse IgG agarose for 1 h at 4 °C with end-over-end mixing; the lysate was then precleared a second time by overnight incubation with IgG agarose. After preclearing, the lysate was incubated with FLAG-agarose for 2 h at 4 °C with end-over-end mixing, and the beads were washed three times (15 min each, 4 °C) with 25 mM Tris and 100 mM NaCl (pH 7.4). FLAG-CFP-Asef2 protein was eluted from the beads by incubation with 0.2 mg/mL FLAG peptide suspended in 25 mM Tris and 100 mM NaCl (pH 7.4) for 30 min at 4 °C; this elution was repeated, and the eluates were pooled. The eluate was subjected to sodium dodecyl sulfate-polyacrylamide gel electrophoresis (SDS-PAGE) on a 10% slab, followed by staining with Coomassie Brilliant Blue R-250 (EMD Millipore, Billerica, MA) to determine the protein purity.

To examine serine phosphorylation, HEK293 cells from a single 150 mm dish per condition were transfected with 8 µg of either FLAG-CFP or FLAG-CFP-Asef2 cDNAs and were immunoprecipitated using the aforementioned protocol. The eluates were subjected to SDS-PAGE and transferred to nitrocellulose membranes. Membranes were incubated with either phosphoserine polyclonal antibody or M2 FLAG monoclonal antibody, followed by incubation with AlexaFluor 680 antirabbit IgG (Life Technologies, Grand Island, NY) or IRDye 800 antimouse IgG (Rockland Immunochemicals Inc., Gilbertsville, PA). Membranes were scanned with a LI-COR Odyssey Infrared Imaging System (LI-COR Biosciences, Lincoln, NE).

Enzymatic Proteolysis

Purified Asef2 was separated into three aliquots containing equal amounts of protein and was subjected to enzymatic digestion using trypsin, chymotrypsin, and Glu-C proteases (Promega, Madison, WI), as described previously.²⁹ Briefly, approximately 5 µg of purified Asef2 was resuspended in 75 µL of 25 mM ammonium bicarbonate and was aliquoted into three 25 µL samples containing approximately 1.7 µg of protein. Reduction and alkylation of cysteine sulfhydryl groups were performed by the addition of 1.5 µL of 45 mM dithiothreitol

(DTT) and incubation for 30 min at 55 °C, followed by the addition of 2.5 μ L of 100 mM iodoacetamide (IAM) and incubation in darkness for 30 min at room temperature. Digestion was performed by adding 42 ng of trypsin, chymotrypsin, or Glu-C at a ratio of 1:40 protease/protein (w/w), followed by incubation at 37 °C for 16, 4, and 6 h, respectively. To quench proteolysis, 1 μ L of 88% formic acid was added. The digested material was lyophilized and reconstituted in 25 μ L of 0.1% formic acid for LC–MS analysis.

Two additional trypsin digestions were performed at strongly denaturing conditions using heat and organic solvent. Both samples contained approximately 2 μ g of purified and aliquoted protein. For denaturation by heat, the sample was reconstituted with 25 mM ammonium bicarbonate and denatured for 15 min at 90 °C. For denaturation by high organic solvent, the respective sample was reconstituted with 20 μ L of acetonitrile (HPLC grade) and 5 μ L of 25 mM ammonium bicarbonate to achieve a solution of 80% acetonitrile.^{30,31} Both samples were treated with DTT and IAM as described above to reduce and alkylate cysteine sulfhydryl groups. Digestion was performed by adding 52 ng (1:40 protease/protein, w/w) of trypsin (Promega, Madison, WI) to each sample. The high organic solvent digestion (referred to as Trypsin^{Org}) was stopped after 1 h of incubation at 37 °C, while the high temperature denatured digestion (referred to as Trypsin^{Temp}) was allowed to proceed for 16 h at 37 °C. The digestions were quenched, dried, and reconstituted as described above.

LC–MS/MS

Initial digestions of Asef2 were loaded onto a reverse-phase capillary trap column using a helium-pressurized cell (pressure bomb). The trap column (360 μ m OD \times 150 μ m ID) was fitted with a filter end-fitting (IDEX Health & Science, Oak Harbor, WA) and packed with 4 cm of C18 reverse phase material (Jupiter, 5 μ m beads, 300 Å; Phenomenex, Torrance, CA). After sample loading, an M-520 microfilter union (IDEX Health & Science) was used to connect the trap column to a capillary analytical column (360 μ m OD \times 100 μ m ID) equipped with a laser-pulled emitter tip and was packed with 20 cm of C18 material (Jupiter, 3 μ m beads, 300 Å; Phenomenex, Torrance, CA). Peptides were gradient-eluted at a flow rate of 500 nL/min using an Eksigent NanoLC Ultra HPLC, and the mobile phase solvents consisted of 0.1% formic acid, 99.9% water (solvent A) and 0.1% formic acid, 99.9% acetonitrile (solvent B). The gradient consisted of the following: 2–45% B in 40 min, 45–90% B in 10 min, 90% B for 5 min, 90–2% B in 10 min. Subsequent trypsin digestions of Asef2 were loaded directly onto the capillary analytical column using the Eksigent NanoLC Ultra HPLC and autosampler, and the same reverse phase gradient was performed. Upon gradient-elution, peptides were mass analyzed on a LTQ Orbitrap Velos mass spectrometer (Thermo Scientific, San Jose, CA) equipped with a nanoelectrospray ionization source. The instrument was operated using a data-dependent method with dynamic exclusion enabled. Full scan (m/z 300–2000) spectra were acquired with the Orbitrap as the mass analyzer (resolution 60 000), and the top 10 most abundant ions in each MS scan were selected for fragmentation in the LTQ. An isolation width of 2 m/z , activation time of 10 ms, and normalized collision energy of 35% were used to generate MS/MS spectra. The MSⁿ AGC target value was set to 1×10^4 , and the maximum injection time was 100 ms.

Bioinformatics

For peptide identification, tandem mass spectra were converted into DTA files using Scansifter and searched using a custom version of SEQUEST (Thermo Fisher Scientific, San Jose, CA) on the Vanderbilt ACCRE Linux cluster against a concatenated forward and reversed (decoy) database containing the *Homo sapiens* subset of the UniProtKB (www.uniprot.org) protein database, which was appended with the Asef2 sequence containing the PCR fragment “IRL” prior to the N-terminus methionine (shown in Supporting Information) for improved coverage of the N-terminus of Asef2. The chymotrypsin digestion was searched with nonspecific protease conditions. A maximum of three missed cleavages was allowed for trypsin digests, where cleavage was restricted to the C-terminal side of arginine (R) and lysine (K) residues, and six missed cleavages were allowed for Glu-C with cleavage restricted to the C-terminal side of glutamic acid (E) residues. Spectra were searched using a 2.5 Da mass tolerance for the precursor peptide mass, and parameters were set to search for monoisotopic masses of the product ions. Allowable variable modifications were limited to carbamidomethyl derivatization of cysteine, oxidation of methionine, and phosphorylation of serine, tyrosine, and threonine. Scaffold version 4.3.2 (Proteome Software Inc., Portland, OR) was used to visualize and validate peptide and protein identifications based on MS/MS data. A minimum probability threshold of 95% was required for peptide identifications; however, most peptides achieved probabilities of 99% or greater. For protein identification, the minimum requirements were four identified peptides per protein and a protein probability threshold of 99%.^{32,33} For all samples, the decoy false discovery rates (FDR) were 0.0% at the protein level and 0.00% at the peptide level. Identifications made to Asef2 were based on the sequence associated with accession number A2VEA_HUMAN, and Asef2 was identified in all samples with 100% probability. All potential peptides and phosphopeptides achieving the minimum probability threshold were manually validated, and MS/MS spectra for all peptides are provided in the Supporting Information. Additionally, several peptides not found by the bioinformatics were manually identified and validated. These peptides are noted in the Supporting Information, as well.

Migration Analysis and Microscopy

HT1080 cells were transfected with 1.5 μ g of GFP, GFP-Asef2, GFP-Asef2-S106A, or GFP-Asef2-S106D cDNAs and were incubated for 24 h at 37 °C. Subsequently, the cells were plated on tissue culture dishes that were coated with 5 μ g/mL fibronectin (diluted in Dulbecco's Phosphate Buffered Saline (DPBS, Life Technologies, Grand Island, NY)) and allowed to adhere for 1 h at 37 °C. Prior to imaging, the culture medium was replaced with SFM4MAB medium (Hyclone, Logan, UT) supplemented with 2% FBS. Images were obtained every 5 min for 6 h using an inverted Olympus IX71 microscope (Melville, NY) with a Retiga EXi CCD camera (QImaging, Surrey, BC), a 10 \times objective (NA 0.3), and MetaMorph software (Molecular Devices, Sunnyvale, CA) connected to a Lambda 10-2 automated controller (Sutter Instruments, Novato, CA). GFP-expressing cells were visualized with an Endow GFP Bandpass filter cube (excitation HQ470/40, emission HQ525/50, Q495LP dichroic mirror) (Chroma, Brattleboro, VT). MetaMorph software was used to track cell movement, and the migration speed was calculated by dividing the net distance traveled (μ m) by the migration time (h). Wind-Rose plots were

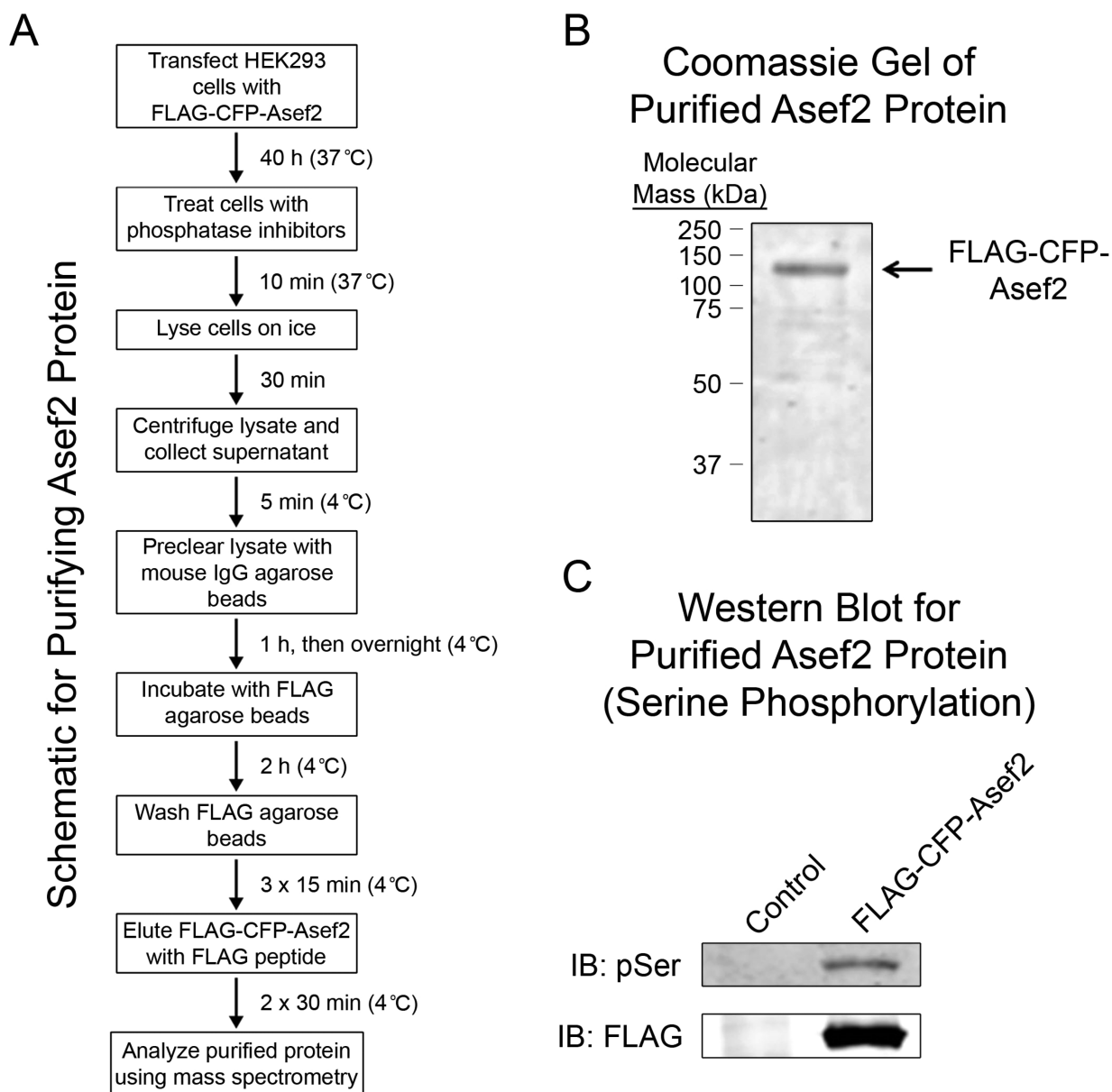


Figure 1. Purification of FLAG-CFP-Asef2. (A) Schematic showing the protocol used to purify FLAG-CFP-Asef2 for LC–MS analysis. (B) SDS-PAGE gel of immunoprecipitated FLAG-CFP-Asef2 that was stained with Coomassie Blue. The arrow points to the band representing purified FLAG-CFP-Asef2 in the eluted sample. (C) Purified FLAG-CFP (control) and FLAG-CFP-Asef2 were subjected to SDS-PAGE, followed by immunoblotting (IB) with phosphoserine (pSer, upper panel) and FLAG (lower panel) antibodies. These panels show that FLAG-CFP-Asef2 is phosphorylated on serine residues.

generated as previously described.³⁴ SPSS Statistics, version 22 (Armonk, NY), was used for statistical analyses of migration, adhesion turnover, and Rac activity assays. One-way ANOVA was performed to compare multiple means, followed by post hoc tests (Games-Howell pairwise comparison tests) to determine the level of significance ($p < 0.05$).

Adhesion Turnover Assay

HT1080 cells were cotransfected with 1.5 μg of mCherry-paxillin cDNA and 1.5 μg of either GFP, GFP-Asef2, GFP-Asef2-S106A, or GFP-Asef2-S106D cDNAs and were incubated for 24 h. Cells were then plated on glass-bottom dishes coated with fibronectin (5 $\mu\text{g}/\text{mL}$) and were allowed to adhere for 1 h at 37 °C. Fluorescent time-lapse images were acquired at 15 s intervals for 20 min using the Olympus IX71 microscope setup described above with a PlanApo 60X OTIRM objective (NA

1.45) and Metamorph software. mCherry was visualized with a TRITC/Cy3 cube (excitation HQ545/30, emission HQ610/75, Q570LP dichroic mirror). The $t_{1/2}$ values for adhesion assembly and disassembly were measured as previously described.^{7,22}

Rac Activity Assay

The Rac binding domain (termed p21-binding domain, or PBD) from the effector p21-activated kinase (PAK) was tagged with glutathione-S-transferase (GST), expressed, and attached to glutathione sepharose beads as previously described.³⁵ HT1080 cells were cultured on 60 mm tissue culture dishes coated with 5 $\mu\text{g}/\text{mL}$ fibronectin and cotransfected with 2 μg of FLAG-Rac1 cDNA and 4 μg of either GFP, GFP-Asef2, GFP-Asef2-S106A, or GFP-Asef2-S106D cDNAs. After 24 h, cells were lysed and assayed for Rac activity as previously

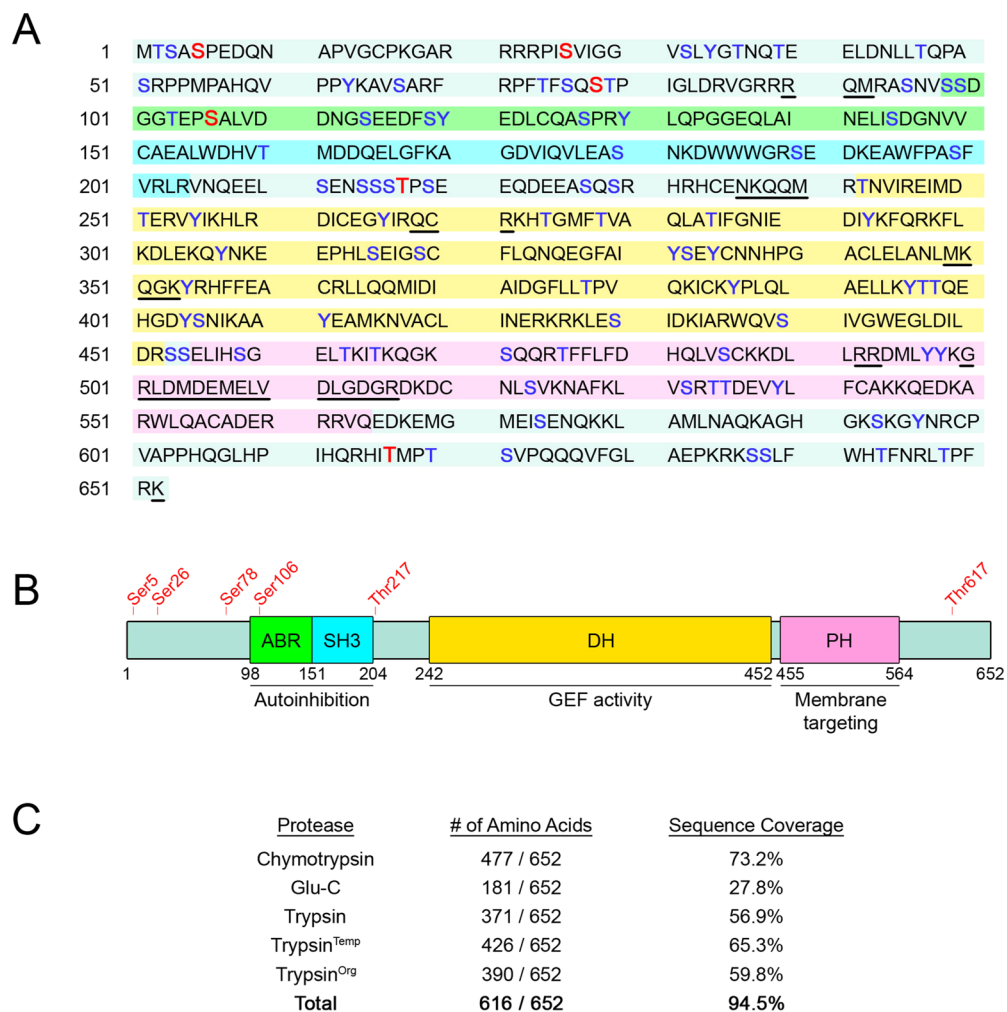


Figure 2. Phosphorylation sites identified in Asef2. (A) The protein sequence of Asef2 is shown with the phosphorylation sites that were detected by LC–MS/MS in red. Serine, threonine, and tyrosine residues that did not have detectable phosphorylation are shown in blue. Colored shading represents the conserved domains in Asef2 as shown in panel B. Underlined residues were not detected in the MS analyses. (B) Schematic of Asef2 showing conserved domains and the location of the six identified phosphorylation sites (red). The domain numbering is based on Kawasaki et al.²¹ (C) Summary of Asef2 amino acid sequence coverage by LC–MS/MS analyses. Purified Asef2 samples were treated with multiple proteases (trypsin, chymotrypsin, or Glu-C) to achieve high sequence coverage. Additional trypsin digestions were performed with strongly denaturing conditions, which included high temperature (90 °C, Trypsin^{Temp}) or a high percentage of organic solvent (80% acetonitrile, Trypsin^{Org}), to obtain sequence coverage of regions that were resistant to trypsin under standard digestion conditions.

described.^{34,35} Briefly, cells were lysed with 50 mM Tris, 1% NP-40, 10% glycerol, 100 mM NaCl, 2 mM MgCl₂, and a protease inhibitor cocktail, pH 7.5 (lysis buffer). A small fraction of each lysate was kept to determine the amount of total Rac. The remaining lysate was incubated with GST-PBD beads for 1 h at 4 °C with end-over-end mixing. The beads were washed three times with lysis buffer. Then, the bound protein was eluted from the beads with Laemmli sample buffer and analyzed via Western blot. The amount of active Rac pulled down was normalized to total Rac for each condition.

RESULTS AND DISCUSSION

Identification of Phosphorylation Sites in Human Asef2

Because Asef2 phosphorylation, which could be an important regulatory mechanism for the activity and function of this protein, had not been previously investigated, we utilized an LC–MS/MS-based approach to uncover potential phosphorylation sites in Asef2.²⁹ To perform MS analyses, FLAG-CFP-Asef2 was expressed in HEK293 cells and then purified

according to the immunoprecipitation protocol outlined in Figure 1A.²⁹ A predominant band with a molecular mass corresponding to that of FLAG-CFP-Asef2 was observed when the immunoprecipitated protein sample was subjected to SDS-PAGE followed by Coomassie Blue staining (Figure 1B). This band was confirmed to be FLAG-CFP-Asef2 via Western blot analysis (Figure 1C). We next examined the phosphorylation state of Asef2 by using a phosphoserine antibody; a distinct band was observed for the Asef2 sample compared to the control sample (FLAG-CFP), demonstrating that Asef2 is phosphorylated on serine residues (Figure 1C). Collectively, these results indicate that the immunoprecipitated protein sample is suitable for MS analysis to identify specific phosphorylated residues in Asef2.

Multiple proteases were used to obtain complete coverage of the potential sites of phosphorylation in Asef2. Initially, trypsin, chymotrypsin, and Glu-C digestions were used, providing partial (86%) sequence coverage, with 93% coverage of serine, threonine, and tyrosine residues. However, two significant stretches of the Asef2 protein sequence from R492-K518 and

Table 1. Phosphorylation Sites Identified in Asef2 by LC–MS/MS Analysis

peptide ^a	sequence position	protease ^b	<i>m/z</i> ^c (charge)	mass error (ppm)
–LMTSApSPEDQNAPVGC*PK ¹⁷	S5	Trypsin ^{Org}	991.42 (+2)	0.91
² TSApSPEDQNAPVGC*PK ¹⁷	S5	Chymo	869.36 (+2)	–1.27
²² RRIPpSVIGGVSLYGTNQTEELDNLLTQPASRPPMPAHQVPPYK ⁶⁴	S26	Trypsin ^{Org}	962.30 (+5)	1.77
²³ RIPpSVIGGVSLYGTNQTEELDNLLTQPASRPPMPAHQVPPYK ⁶⁴	S26	Trypsin ^{Temp}	1163.59 (+4)	0.52
²³ RIPpSVIGGVSLYGTNQTEELDNLLTQPASRPPMPAHQVPPYK ⁶⁴	S26	Trypsin ^{Org}	1163.59 (+4)	2.49
⁷⁰ FRPFTFSQpSTPIGLDR ⁸⁵	S78	Trypsin	650.32 (+3)	0.92
⁷⁰ FRPFTFSQpSTPIGLDR ⁸⁵	S78	Trypsin ^{Temp}	650.32 (+3)	0.77
⁷⁰ FRPFTFSQpSTPIGLDR ⁸⁵	S78	Trypsin ^{Org}	650.32 (+3)	2.00
⁷⁰ FRPFTFSQpSTPIGLDRVGR ⁸⁸	S78	Trypsin ^{Org}	566.04 (+4)	0.53
⁷⁰ FRPFTFSQpSTPIGLDRVGR ⁸⁹	S78	Trypsin ^{Org}	605.06 (+4)	0.66
⁹⁴ ASNVSSDGGTEpSALVDDNGSEEDFSYEDLC*QASPR ¹²⁹	S106	Trypsin	1295.86 (+3)	–0.23
⁹⁴ ASNVSSDGGTEpSALVDDNGSEEDFSYEDLC*QASPR ¹²⁹	S106	Trypsin ^{Temp}	1295.86 (+3)	–0.39
⁹⁴ ASNVSSDGGTEpSALVDDNGSEEDFSYEDLC*QASPR ¹²⁹	S106	Trypsin ^{Org}	1295.86 (+3)	1.00
²⁰⁵ VNQEELSENSSpTPSEEQDEEASQSR ²³⁰	T217	Trypsin	992.73 (+3)	–0.40
²⁰⁵ VNQEELSENSSpTPSEEQDEEASQSR ²³⁰	T217	Trypsin ^{Temp}	992.73 (+3)	0.71
²⁰³ LRVNQEELSENSSpTPSEEQDEEASQSR ²³⁰	T217	Trypsin ^{Org}	1082.46 (+3)	0.00
²¹⁰ LENSSSpTPSEEQDEEASQSRHRHC*E ²³⁵	T217	Glu-C	774.81 (+4)	–0.26
⁶¹⁵ HIPtMPTSVpQQVFLAEPK ⁶³⁴	T617	Trypsin ^{Org}	763.38 (+3)	1.18

^aThe hyphen “–” indicates that the peptide occurs at the N-terminus of Asef2 and includes a residual PCR fragment leucine (L) prior to the start of Asef2; the “p” denotes a site of phosphorylation; an asterisk “*” denotes carboxyamidomethylation of cysteine. ^b“Chymo” refers to digestion using chymotrypsin. The superscript “Org” denotes sample denatured by a high percentage of organic solvent; the superscript “Temp” denotes sample denatured by heat. ^cThe *m/z* values shown here are truncated to two decimal places; however, mass errors were calculated with *m/z* values extended to four decimal places. The *m/z* values used in the mass error calculations may be found in the Supporting Information.

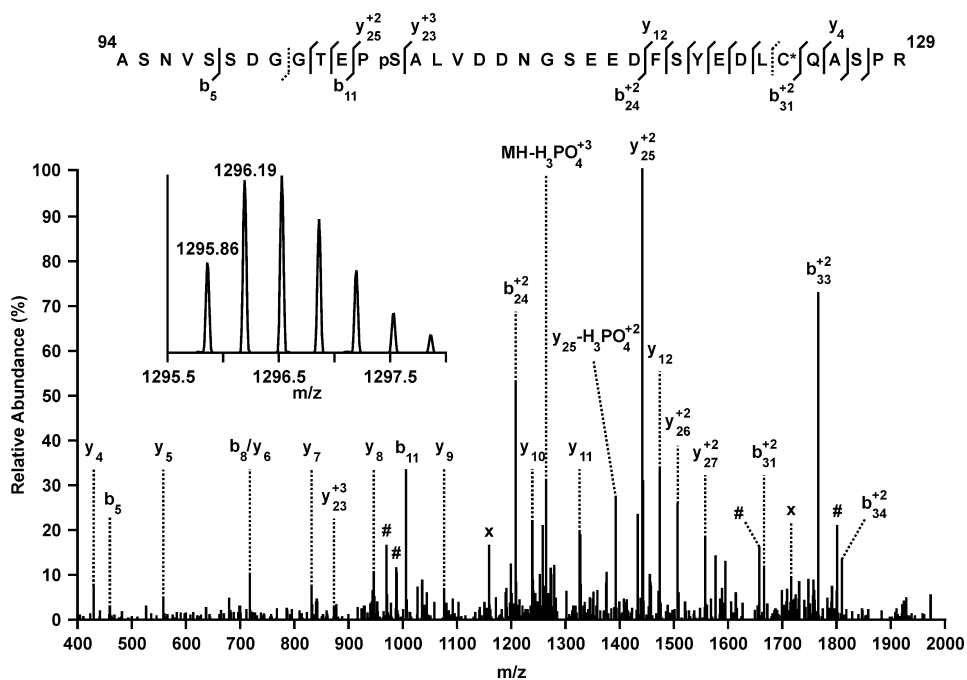


Figure 3. MS and MS/MS spectra for an Asef2 phosphorylated peptide. Data-targeted MS/MS scan of *m/z* 1295.86 in the Trypsin^{Org} sample, corresponding to the triply charged (inset) phosphopeptide ⁹⁴ASNVSSDGGTEpSALVDDNGSEEDFSYEDLC*QASPR¹²⁹. All backbone cleavages (b and y ions) observed are marked on the sequence (top), and additional ions are labeled in the spectrum. Sequence positions for *b*₈ and *y*₆ are shown with dashed markers (top) due to isobaric *m/z* values of 718.3. “C*” denotes a carbamidomethyl-modified cysteine. “#” indicates ions corresponding to –H₂O from *b*₁₁⁺(2), *b*₃₁⁺, and *b*₃₄⁺, respectively. “X” denotes ions corresponding to –H₃PO₄ from *b*₂₄⁺ and *b*₃₃⁺, respectively.

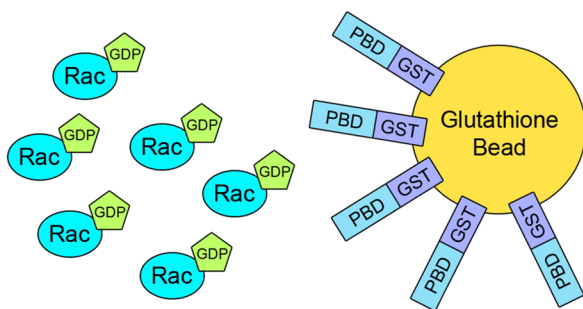
R561–Y596 (Figure 2A) were not covered in the trypsin, chymotrypsin, or Glu-C digestions. These regions have a high abundance of aspartic acid and glutamic acid residues, and therefore may not provide peptides of suitable length for LC–MS analysis upon digestion with Glu-C. While these amino acid sequences have multiple lysine and arginine residues, regions

R492–K518 and R561–Y596 were found to be inaccessible or resistant to trypsin and chymotrypsin under standard digestion conditions.

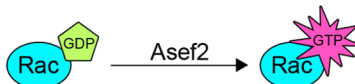
In order to obtain sequence coverage of regions R492–K518 and R561–Y596 of Asef2, additional trypsin digestions were performed using two strongly denaturing approaches: heat and

Schematic for Rac Activity Assay

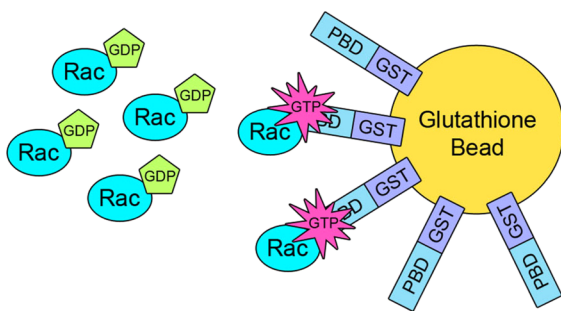
A i. The GST-bound p21-binding domain (PBD) does not bind inactive (GDP-bound) Rac.



ii. Asef2 activates Rac by catalyzing the exchange of GDP for GTP.



iii. Active (GTP-bound) Rac binds to the PBD, allowing both to be precipitated with the glutathione beads.



iv. After elution from the beads, active Rac can be assayed via Western blot.

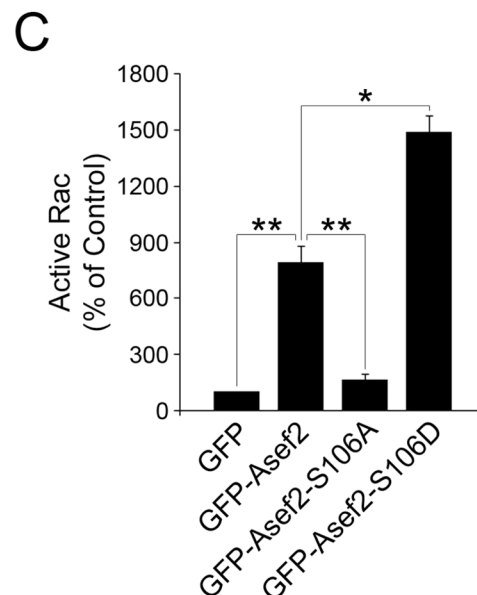
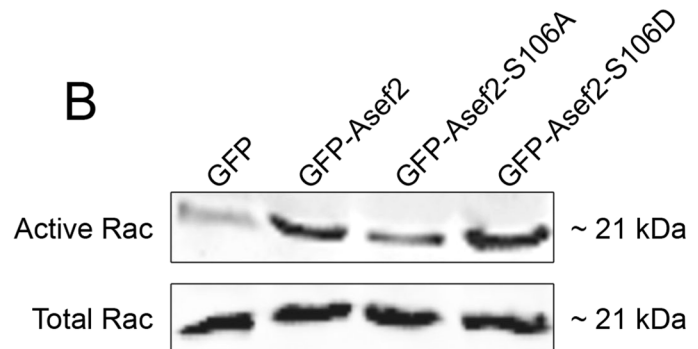


Figure 4. Phosphorylation of S106 stimulates Asef2 GEF activity. (A) Schematic depicting the protocol used to detect active Rac (Rac activity assay), which was modified from Kraus et al.³⁵ (B) HT1080 cells were cotransfected with FLAG-Rac1 cDNA and either GFP, GFP-Asef2, GFP-Asef2-S106A, or GFP-Asef2-S106D, and active Rac was subsequently pulled down from lysates from these cells. The amount of total Rac is shown as a control. (C) Quantification of the amount of active Rac from 3 to 7 separate experiments is shown. Error bars represent s.e.m. * $p = 0.007$, ** $p = 0.001$.

high organic solvent concentration. Digestions done in mixed aqueous–organic solvent conditions have been demonstrated to increase peptide identifications from proteolysis-resistant proteins, while simultaneously allowing for shorter digestion times.^{30,31} Our results showed that an additional 44 residues were covered in regions R492-K518 and R561-Y596 with the strongly denaturing digestions, which were observed as the following peptides: ⁴⁹⁴DMLYYK⁴⁹⁹ and ⁵¹⁷DKDCNLSVK⁵²⁵ in the Trypsin^{Heat} digestion, and ⁵⁶³VQEDKEMGMEISENQ-KKLAMLNAQK⁵⁸⁷, ⁵⁸⁸AGHGKSKGYNRCVPVAPPHQGLHP-IHQK⁶¹⁴, and ⁵⁵²WLQACADERRR⁵⁶² in the Trypsin^{Org} digestion, where the italicized portions contributed to the 44 additional residues observed. Of these 44 amino acids, approximately 64% were observed in the high organic solvent digestion (Trypsin^{Org}). Combined, the two strongly denaturing digestions yielded nearly 82% sequence coverage and accessed additional regions of Asef2 compared to the more conventional, aqueous-based digestions. A sequence coverage of 94.5% was achieved with the five different digestions (Figure 2C), and

complete coverage of the serine, threonine, and tyrosine residues was obtained in the identified peptides.

The identified phosphopeptides are shown in Table 1, along with the type of enzymatic digestion used and the associated mass error. Phosphopeptide identities were initially revealed by SEQUEST, but each was manually validated to confirm the location of phosphorylation. Four sites of phosphorylation were identified in the digestions using standard conditions: pS5, pS78, pS106, and pT217. Two additional sites, pS26 and pT617, were identified from the strongly denatured digestions. Five (pS5, pS26, pS78, pS106, and pT217) of the six total sites of phosphorylation were observed in multiple digests. An example of MS/MS data for the phosphorylated peptide, ⁹⁴ASNVSDDGGTEPpSALVDDNGSEEDFSYEDLCQASPR¹²⁹ is shown in Figure 3. This peptide was conserved in all three tryptic digests, and the observation of both y_{23}^{+3} and y_{25}^{+2} enabled the exact site of phosphorylation (pS106) to be discerned.

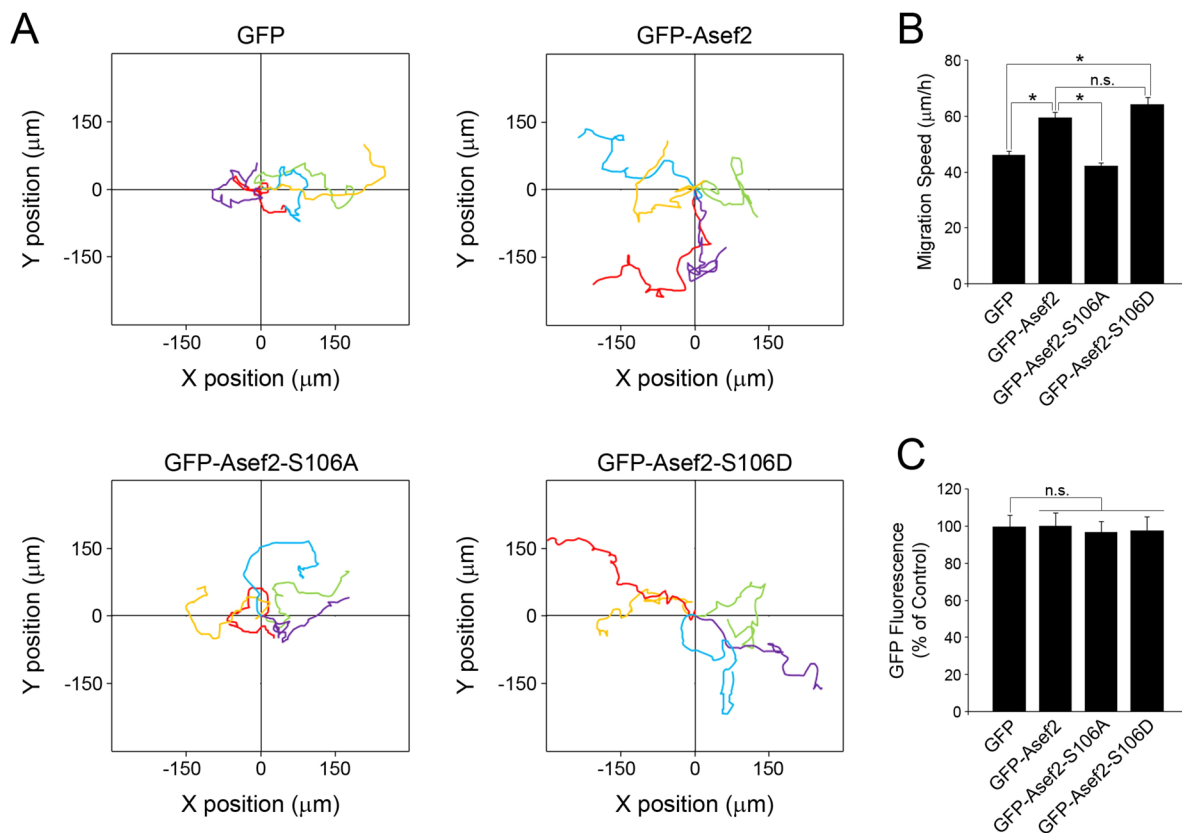


Figure 5. Phosphorylation of S106 is critical for Asef2-promoted cell migration. (A) HT1080 cells expressing GFP, GFP-Asef2, GFP-Asef2-S106A, or GFP-Asef2-S106D were plated on fibronectin-coated dishes and imaged using time-lapse microscopy. The migration of individual cells was tracked and analyzed. Wind-Rose plots depicting the migration tracks for individual cells are shown. (B) Migration speed was quantified for GFP-, GFP-Asef2-, GFP-Asef2-S106A-, and GFP-Asef2-S106D-expressing cells. Error bars represent s.e.m. for 66–159 cells from 4 to 9 independent experiments (*, $p < 0.001$). (C) Quantification of the fluorescence intensity in cells transfected with the indicated cDNAs shows that all the constructs were expressed at comparable levels. Error bars represent s.e.m. for 69–76 cells from 3 separate experiments. For panels B and C, “n.s.” denotes no statistically significant difference.

Serine Phosphorylation Stimulates Asef2 GEF Activity

A majority of the confirmed phosphorylation sites in Asef2 are concentrated at the N-terminus (Figure 2B). One residue (S106) is in the ABR domain, while four others (S5, S26, S78, and T217) bracket the adjacent ABR-SH3 domains. The sixth phosphorylation site (T617), conversely, resides in the C-terminus of Asef2 (Figure 2B). Of these six phosphorylation sites, S106 was particularly intriguing because of its location in the ABR domain, which is a critical region for Asef2 activation.^{20,21} This led us to hypothesize that phosphorylation of S106 is an important regulatory mechanism for Asef2 GEF activity. To investigate the effect of S106 phosphorylation on Asef2 activity, we mutated this residue to either alanine (S106A) or aspartic acid (S106D) using site-directed mutagenesis; these substitutions represent non-phosphorylatable and phosphomimetic analogues, respectively.^{36–38} Then, we assessed the effect of S106 mutation on the activation of the small GTPase Rac using a GTPase activity assay.^{22,34} In this assay, the GST-tagged binding domain from the Rac effector PAK (GST-PBD) is used to detect the active form of Rac from lysates of GFP- and GFP-Asef2-expressing cells (Figure 4A). As expected, expression of wild-type Asef2 caused a significant increase in the level of active Rac (Figure 4B). Quantification showed that the amount of active Rac was increased approximately 8-fold in GFP-Asef2-expressing cells compared with control cells expressing GFP (Figure 4C). In contrast,

GFP-Asef2-S106A expression caused an approximately 80% decrease in active Rac compared to expression of GFP-Asef2 (Figure 4B,C), suggesting that phosphorylation of Asef2 at S106 promotes its GEF activity toward Rac. Expression of GFP-Asef2-S106D resulted in an approximately 2-fold increase in active Rac compared to expression of GFP-Asef2 (Figure 4B,C). Therefore, these results point to S106 as an important phosphorylation site in Asef2 that mediates its ability to activate Rac.

S106 Phosphorylation Regulates Cell Migration

We have previously shown that Asef2 promotes the migration of HT1080 cells plated on fibronectin via active Rac.²² In this study, we demonstrate that phosphorylation of S106 is critical for Asef2-mediated activation of Rac. This led us to hypothesize that S106 phosphorylation of Asef2 plays a role in regulating cell migration. To test this hypothesis, we transfected HT1080 cells with either GFP, GFP-Asef2, GFP-Asef2-S106A, or GFP-Asef2-S106D cDNAs and then plated the cells on fibronectin-coated dishes and assessed cell migration using live-cell imaging. Migration data were generated by tracking individual cells and were used to calculate the migration speed. Figure 5A shows the individual tracks of GFP-, GFP-Asef2-, GFP-Asef2-S106A-, and GFP-Asef2-S106D-expressing cells. The migration paths of GFP-Asef2-expressing cells were significantly longer than those of control cells expressing GFP. Quantification showed an approximately 1.3-fold increase in migration speed

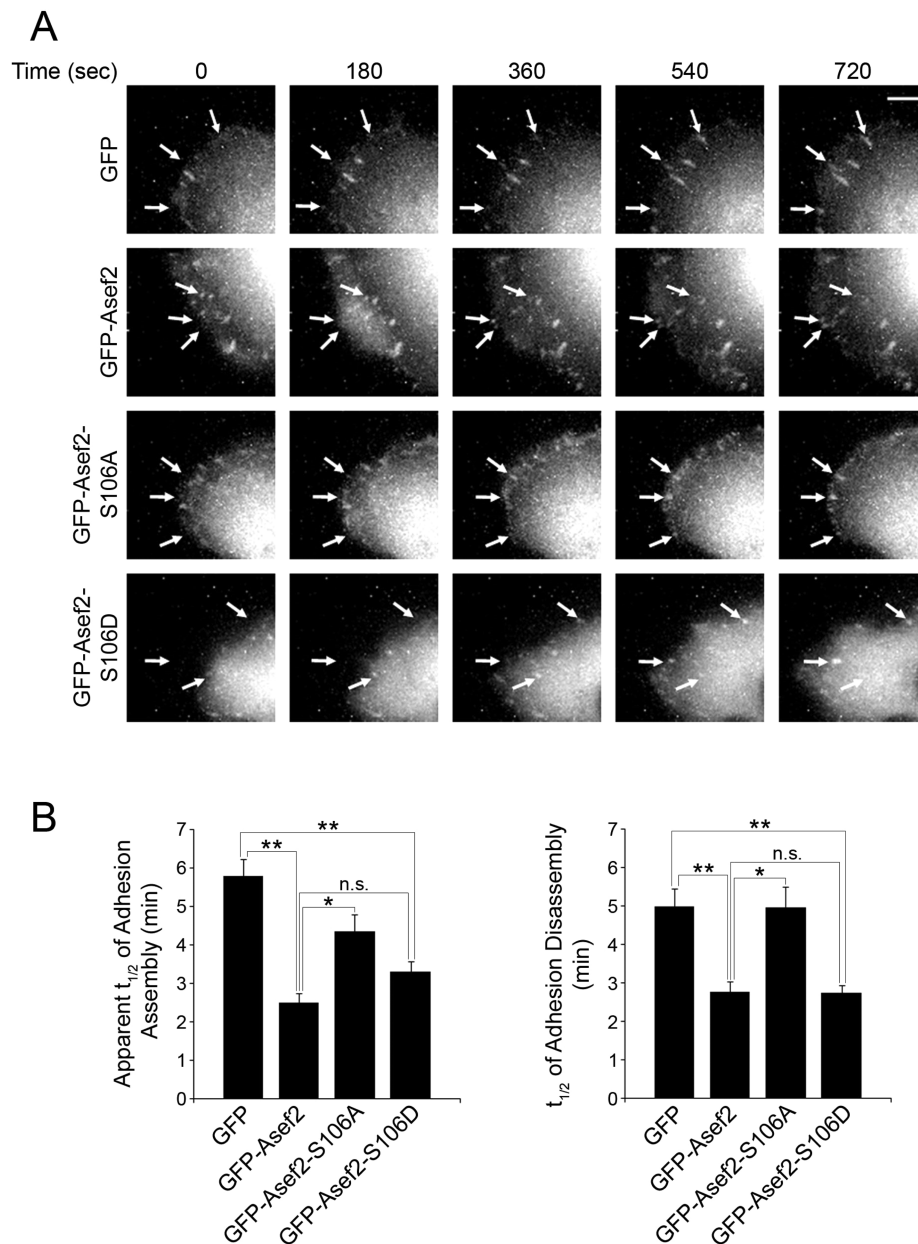


Figure 6. S106 phosphorylation regulates adhesion turnover. (A) HT1080 cells were cotransfected with mCherry-paxillin cDNA and either GFP, GFP-Asef2, GFP-Asef2-S106A, or GFP-Asef2-S106D cDNAs and were subsequently used in adhesion turnover assays. Time-lapse images show adhesions that are assembling and disassembling at the leading edge of migrating cells (arrows). Bar = 5 μ m. (B) Quantification of the apparent $t_{1/2}$ of adhesion assembly and the $t_{1/2}$ of adhesion disassembly for transfected cells is shown. Error bars represent s.e.m. for 34–70 adhesions, which were analyzed in 11–22 cells from 3 to 6 independent experiments (* p < 0.005, ** p < 0.001). “n.s.” denotes no statistically significant difference.

in GFP-Asef2-expressing cells compared to those expressing GFP (Figure 5B). Intriguingly, mutation of serine 106 to alanine abolished this increase in migration (Figure 5B). The migration speed of GFP-Asef2-S106A-expressing cells was significantly decreased compared to cells expressing GFP-Asef2, suggesting that S106 phosphorylation is important for Asef2-promoted cell migration. All of the GFP-tagged proteins were expressed at similar levels (Figure 5C), indicating that changes in migration speed were not due to differential protein expression. Expression of the phosphomimetic S106D mutant resulted in an increase in migration speed compared to that observed with GFP expression (Figure 5B). However, the migration speed of cells expressing GFP-Asef2-S106D was not significantly different than the migration speed of GFP-Asef2-

expressing cells. This result is somewhat unexpected, given the additional increase in Rac activity detected in the GFP-Asef2-S106D-expressing cells (Figure 4C). The expression of wild-type Asef2 may be sufficient to maximally stimulate Asef2 signaling, at least in terms of promoting cell migration. Specifically, the high level of active Rac resulting from wild-type Asef2 expression could be adequate to saturate downstream signaling; thus, a further increase in active Rac, such as that caused by GFP-Asef2-S106D expression, would not yield a higher migration speed. Consistent with this, a previous study showed that expression of constitutively active Rac did not cause a further increase in migration speed compared to that observed with wild-type Rac expression.³⁹ Nevertheless, these

results underscore the importance of S106 phosphorylation in regulating Asef2-mediated cell migration.

Phosphorylation of S106 Modulates Adhesion Turnover

Because the ability of cells to migrate efficiently is dependent on the proper assembly and disassembly of their adhesions (adhesion turnover), and because Asef2-Rac signaling plays an important role in regulating adhesion dynamics,^{7,11,22} S106 phosphorylation may affect migration by modulating adhesion turnover. Therefore, we coexpressed mCherry-paxillin, a well-characterized adhesion marker, with GFP, GFP-Asef2, GFP-Asef2-S106A, or GFP-Asef2-S106D in HT1080 cells and analyzed adhesion turnover using an adhesion turnover assay that we previously developed.^{7,22} In this assay, mCherry-paxillin-containing adhesions from these cells were imaged using time-lapse microscopy (Figure 6A), and the change in fluorescence intensity in individual adhesions was used to calculate $t_{1/2}$ values for adhesion assembly and disassembly. Cells expressing GFP-Asef2 exhibited an approximately 50% decrease in the $t_{1/2}$ values for adhesion assembly and disassembly compared to GFP-expressing cells (Figure 6B); this suggests that adhesions in GFP-Asef2-expressing cells turn over more quickly, resulting in faster cell migration speeds.²² Conversely, the $t_{1/2}$ values for both adhesion assembly and disassembly were significantly larger in GFP-Asef2-S106A-expressing cells compared to those cells expressing GFP-Asef2 (Figure 6B). These data are consistent with the slower cell migration speed that was observed in GFP-Asef2-S106A-expressing cells (Figure 5B), further emphasizing the importance of phosphorylation of this residue for efficient cell migration. Expression of the S106D mutant, on the other hand, resulted in $t_{1/2}$ values that were comparable to those observed with GFP-Asef2 expression. Collectively, these results suggest that the phosphorylation of Asef2 at S106 promotes faster adhesion turnover, which is critical for proficient cell migration.

CONCLUSIONS

Asef2 is emerging as an important GEF in modulating cellular processes, such as migration and adhesion dynamics; however, the mechanisms that regulate the activity and function of Asef2 are currently not well understood. In this study, we identified six phosphorylation sites in Asef2 by LC-MS/MS analysis. We demonstrate that phosphorylation of one of these sites, S106, which is located in the ABR domain, is important for modulating Asef2 GEF activity as well as for Asef2 function in cell migration and adhesion turnover. Four of the other detected phosphorylation sites (S5, S26, S78, and T217) are congregated toward the N-terminus of Asef2, and it is possible that they contribute to Asef2 regulation and/or function as well. Indeed, the N-terminal location of these phosphorylation sites puts them in a potential position to regulate the autoinhibitory state of Asef2 because this region of the protein contains the ABR-SH3 module, which maintains Asef2 in an autoinhibited, inactive state.²⁰ The sixth phosphorylation site (T617) is located in the C-terminus of Asef2. The C-terminus associates with the ABR-SH3 module to maintain Asef2 in an autoinhibitory state.²⁰ Thus, phosphorylation within this region could also affect Asef2 GEF activity. Furthermore, the C-terminus of Asef2 is involved in mediating protein-protein interactions; for example, Asef2 interacts with the actin-binding protein spinophilin, via this region.⁴⁰ Phosphorylation of T617 could be involved in regulating this association or other

protein-protein interactions. Future studies are needed to determine the significance of these phosphorylation sites on Asef2 activity and function.

ASSOCIATED CONTENT

Supporting Information

MS analysis according to MIAPE-MS standards; MS/MS spectra for all identified peptides and phosphopeptides organized by the digestion samples (Trypsin, Chymotrypsin, Glu-C, Trypsin^{Heat}, Trypsin^{Org}); and an excel file containing the SEQUEST scores, precursor mass and charge, mass error, scan number, sequence and sequence position for all peptides and phosphopeptides. This material is available free of charge via the Internet at <http://pubs.acs.org>.

AUTHOR INFORMATION

Corresponding Authors

*(J.A.M.) Tel: 615-322-1195. Fax: 615-343-1234. E-mail: john.a.mclean@vanderbilt.edu.

*(D.J.W.) Tel: 615-936-8274. Fax: 615-343-6707. E-mail: donna.webb@vanderbilt.edu.

Author Contributions

[○]J.C.E., K.M.H., and J.G.F. have contributed to an equal extent.

Notes

The authors declare no competing financial interest.

ACKNOWLEDGMENTS

The authors thank the Vanderbilt Mass Spectrometry Research Center Proteomics Core Facility for data acquisition on an LTQ Orbitrap Velos mass spectrometer funded by National Institutes of Health (S10RR027714). We are grateful to Lan Hu for assistance in preparing cDNA constructs. This work was supported by National Institutes of Health Grant (NIH) GM092914 (D.J.W.) and in part by National Institutes of Health Grant UH2TR000491 (K.M.H., J.G.F., and J.A.M.), the Defense Threat Reduction Agency HDTRA-09-1-00-13 and DTRA100271 A-5196 (K.M.H., J.G.F., and J.A.M.), the Vanderbilt Institute of Chemical Biology (J.A.M.), and the Vanderbilt Institute for Integrative Biosystems Research and Education (D.J.W. and J.A.M.).

ABBREVIATIONS

ABR, APC-binding region; APC, adenomatous polyposis coli; DH, Dbl homology; DTT, dithiothreitol; GAP, GTPase activating protein; GEF, guanine nucleotide exchange factor; GST, glutathione-S-transferase; IAM, iodoacetamide; LC, liquid chromatography; MS, mass spectrometry; MS/MS, tandem mass spectrometry; PAK, p21-activated kinase; PBD, p21-binding domain; PH, pleckstrin homology; SDS-PAGE, sodium dodecyl sulfate-polyacrylamide gel electrophoresis; SH3, Src homology 3

REFERENCES

- (1) Vicente-Manzanares, M.; Horwitz, A. R. Cell migration: an overview. *Methods Mol. Biol.* **2011**, *769*, 1–24.
- (2) Yamaguchi, H.; Wyckoff, J.; Condeelis, J. Cell migration in tumors. *Curr. Opin Cell Biol.* **2005**, *17* (5), 559–564.
- (3) Hopkins, P. N. Molecular biology of atherosclerosis. *Physiol Rev.* **2013**, *93* (3), 1317–1542.
- (4) Lauffenburger, D. A.; Horwitz, A. F. Cell migration: a physically integrated molecular process. *Cell* **1996**, *84* (3), 359–369.

- (5) Beningo, K. A.; Dembo, M.; Kaverina, I.; Small, J. V.; Wang, Y. L. Nascent focal adhesions are responsible for the generation of strong propulsive forces in migrating fibroblasts. *J. Cell Biol.* **2001**, *153* (4), 881–888.
- (6) Laukaitis, C. M.; Webb, D. J.; Donais, K.; Horwitz, A. F. Differential dynamics of alpha 5 integrin, paxillin, and alpha-actinin during formation and disassembly of adhesions in migrating cells. *J. Cell Biol.* **2001**, *153* (7), 1427–1440.
- (7) Webb, D. J.; Donais, K.; Whitmore, L. A.; Thomas, S. M.; Turner, C. E.; Parsons, J. T.; Horwitz, A. F. FAK-Src signalling through paxillin, ERK and MLCK regulates adhesion disassembly. *Nat. Cell Biol.* **2004**, *6* (2), 154–161.
- (8) Choi, C. K.; Vicente-Manzanares, M.; Zareno, J.; Whitmore, L. A.; Mogilner, A.; Horwitz, A. R. Actin and alpha-actinin orchestrate the assembly and maturation of nascent adhesions in a myosin II motor-independent manner. *Nat. Cell Biol.* **2008**, *10* (9), 1039–1050.
- (9) Webb, D. J.; Parsons, J. T.; Horwitz, A. F. Adhesion assembly, disassembly and turnover in migrating cells – over and over and over again. *Nat. Cell Biol.* **2002**, *4* (4), E97–100.
- (10) Chrzanowska-Wodnicka, M.; Burridge, K. Rho-stimulated contractility drives the formation of stress fibers and focal adhesions. *J. Cell Biol.* **1996**, *133* (6), 1403–1415.
- (11) Rottner, K.; Hall, A.; Small, J. V. Interplay between Rac and Rho in the control of substrate contact dynamics. *Curr. Biol.* **1999**, *9* (12), 640–648.
- (12) Nobes, C. D.; Hall, A. Rho, rac, and cdc42 GTPases regulate the assembly of multimolecular focal complexes associated with actin stress fibers, lamellipodia, and filopodia. *Cell* **1995**, *81* (1), 53–62.
- (13) Jaffe, A. B.; Hall, A. Rho GTPases: biochemistry and biology. *Annu. Rev. Cell Dev. Biol.* **2005**, *21*, 247–269.
- (14) West, M.; Kung, H. F.; Kamata, T. A novel membrane factor stimulates guanine nucleotide exchange reaction of ras proteins. *FEBS Lett.* **1990**, *259* (2), 245–248.
- (15) Cherfils, J.; Zeghouf, M. Regulation of small GTPases by GEFs, GAPs, and GDIs. *Physiol. Rev.* **2013**, *93* (1), 269–309.
- (16) Trahey, M.; McCormick, F. A cytoplasmic protein stimulates normal N-ras p21 GTPase, but does not affect oncogenic mutants. *Science* **1987**, *238* (4826), 542–545.
- (17) Gibbs, J. B.; Schaber, M. D.; Allard, W. J.; Sigal, I. S.; Scolnick, E. M. Purification of ras GTPase activating protein from bovine brain. *Proc. Natl. Acad. Sci. U. S. A.* **1988**, *85* (14), S026–S030.
- (18) Ridley, A. J.; Hall, A. The small GTP-binding protein rho regulates the assembly of focal adhesions and actin stress fibers in response to growth factors. *Cell* **1992**, *70* (3), 389–399.
- (19) Ridley, A. J.; Paterson, H. F.; Johnston, C. L.; Diekmann, D.; Hall, A. The small GTP-binding protein rac regulates growth factor-induced membrane ruffling. *Cell* **1992**, *70* (3), 401–410.
- (20) Hamann, M. J.; Lubking, C. M.; Luchini, D. N.; Billadeau, D. D. Asef2 functions as a Cdc42 exchange factor and is stimulated by the release of an autoinhibitory module from a concealed C-terminal activation element. *Mol. Cell Biol.* **2007**, *27* (4), 1380–1393.
- (21) Kawasaki, Y.; Sagara, M.; Shibata, Y.; Shirouzu, M.; Yokoyama, S.; Akiyama, T. Identification and characterization of Asef2, a guanine-nucleotide exchange factor specific for Rac1 and Cdc42. *Oncogene* **2007**, *26* (55), 7620–7267.
- (22) Bristow, J. M.; Sellers, M. H.; Majumdar, D.; Anderson, B.; Hu, L.; Webb, D. J. The Rho-family GEF Asef2 activates Rac to modulate adhesion and actin dynamics and thereby regulate cell migration. *J. Cell Sci.* **2009**, *122* (Pt 24), 4535–4546.
- (23) Murayama, K.; Shirouzu, M.; Kawasaki, Y.; Kato-Murayama, M.; Hanawa-Suetsugu, K.; Sakamoto, A.; Katsura, Y.; Suenaga, A.; Toyama, M.; Terada, T.; Taiji, M.; Akiyama, T.; Yokoyama, S. Crystal structure of the rac activator, Asef, reveals its autoinhibitory mechanism. *J. Biol. Chem.* **2007**, *282* (7), 4238–4242.
- (24) Zhang, Z.; Chen, L.; Gao, L.; Lin, K.; Zhu, L.; Lu, Y.; Shi, X.; Gao, Y.; Zhou, J.; Xu, P.; Zhang, J.; Wu, G. Structural basis for the recognition of Asef by adenomatous polyposis coli. *Cell Res.* **2012**, *22* (2), 372–386.
- (25) Walsh, C. T.; Garneau-Tsodikova, S.; Gatto, G. J., Jr. Protein posttranslational modifications: the chemistry of proteome diversifications. *Angew. Chem., Int. Ed. Engl.* **2005**, *44* (45), 7342–7372.
- (26) Kato, J.; Kaziro, Y.; Satoh, T. Activation of the guanine nucleotide exchange factor Dbl following ACK1-dependent tyrosine phosphorylation. *Biochem. Biophys. Res. Commun.* **2000**, *268* (1), 141–147.
- (27) Servitja, J. M.; Marinissen, M. J.; Sodhi, A.; Bustelo, X. R.; Gutkind, J. S. Rac1 function is required for Src-induced transformation. Evidence of a role for Tiam1 and Vav2 in Rac activation by Src. *J. Biol. Chem.* **2003**, *278* (36), 34339–34346.
- (28) Miyamoto, Y.; Torii, T.; Yamamori, N.; Ogata, T.; Tanoue, A.; Yamauchi, J. Akt and PP2A reciprocally regulate the guanine nucleotide exchange factor Dock6 to control axon growth of sensory neurons. *Sci. Signal* **2013**, *6* (265), ra15.
- (29) Gant-Branum, R. L.; Broussard, J. A.; Mahsut, A.; Webb, D. J.; McLean, J. A. Identification of phosphorylation sites within the signaling adaptor APPL1 by mass spectrometry. *J. Proteome Res.* **2010**, *9* (3), 1541–1548.
- (30) Russell, W. K.; Park, Z. Y.; Russell, D. H. Proteolysis in mixed organic-aqueous solvent systems: applications for peptide mass mapping using mass spectrometry. *Anal. Chem.* **2001**, *73* (11), 2682–2685.
- (31) Strader, M. B.; Tabb, D. L.; Herve, W. J.; Pan, C.; Hurst, G. B. Efficient and specific trypsin digestion of microgram to nanogram quantities of proteins in organic-aqueous solvent systems. *Anal. Chem.* **2006**, *78* (1), 125–134.
- (32) Keller, A.; Nesvizhskii, A. I.; Kolker, E.; Aebersold, R. Empirical statistical model to estimate the accuracy of peptide identifications made by MS/MS and database search. *Anal. Chem.* **2002**, *74* (20), 5383–5392.
- (33) Nesvizhskii, A. I.; Keller, A.; Kolker, E.; Aebersold, R. A statistical model for identifying proteins by tandem mass spectrometry. *Anal. Chem.* **2003**, *75* (17), 4646–4658.
- (34) Jean, L.; Majumdar, D.; Shi, M.; Hinkle, L. E.; Diggins, N. L.; Ao, M.; Broussard, J. A.; Evans, J. C.; Choma, D. P.; Webb, D. J. Activation of Rac by Asef2 promotes myosin II-dependent contractility to inhibit cell migration on type I collagen. *J. Cell Sci.* **2013**, *126* (Pt 24), 5585–5597.
- (35) Knaus, U. G.; Bamberg, A.; Bokoch, G. M. Rac and Rap GTPase activation assays. *Methods Mol. Biol.* **2007**, *412*, 59–67.
- (36) Langan, T. A.; Rall, S. C.; Cole, R. D. Variation in primary structure at a phosphorylation site in lysine-rich histones. *J. Biol. Chem.* **1971**, *246* (6), 1942–1944.
- (37) Thorsness, P. E.; Koshland, D. E., Jr. Inactivation of isocitrate dehydrogenase by phosphorylation is mediated by the negative charge of the phosphate. *J. Biol. Chem.* **1987**, *262* (22), 10422–10425.
- (38) Tarrant, M. K.; Cole, P. A. The chemical biology of protein phosphorylation. *Annu. Rev. Biochem.* **2009**, *78*, 797–825.
- (39) Pankov, R.; Endo, Y.; Even-Ram, S.; Araki, M.; Clark, K.; Cukierman, E.; Matsumoto, K.; Yamada, K. M. A Rac switch regulates random versus directionally persistent cell migration. *J. Cell Biol.* **2005**, *170* (5), 793–802.
- (40) Sagara, M.; Kawasaki, Y.; Iemura, S. I.; Natsume, T.; Takai, Y.; Akiyama, T. Asef2 and Neurabin2 cooperatively regulate actin cytoskeletal organization and are involved in HGF-induced cell migration. *Oncogene* **2009**, *28* (10), 1357–1365.